COMPDYN 2013
4th ECCOMAS Thematic Conference on
Computational Methods in Structural Dynamics and Earthquake Engineering
M. Papadrakakis, V. Papadopoulos, V. Plevris (eds.)
Kos Island, Greece, 12–14 June 2013

EXCITATION OF PARAMETRIC RESONANCE IN MICRO BEAMS BY JOULE'S HEATING

Timur Sibgatullin, David Schreiber, Slava Krylov*

Microsystems Design and Characterization Laboratory, School of Mechanical Engineering, Faculty of Engineering, Tel Aviv University, Israel
*e-mail: vadis@eng.tau.ac.il

Keywords: MEMS, double clamped micro beam, Joule's heating, parametric resonance, buckling.

Abstract. *In this work we investigate the feasibility of excitation of parametric resonance in micro/nano beams by means of Joule's heating of the beam's material. A time-dependent voltage applied to the beam's ends generates an alternate electric current through the beam, which results in a time-dependent heating of the beam's material and appearance of a time-dependent compressive axial force acting on the beam. By choosing appropriate values of the frequency and magnitude of the voltage, efficient parametric excitation of the beam can be achieved. The main advantage of the suggested approach is its simplicity and compatibility with the existing fabrication processes and common configurations of micro devices. The beam is modeled in the framework of the Euler-Bernoulli theory. The influence of the thermo-elastic effects on the heat generation is neglected and it is assumed that the contribution of the Joule's heating is dominant. The thermo-mechanical coupling is introduced through the thermal expansion of the beam's material due to the heating. The time-harmonic heat-transfer problem is solved analytically. An approximate single degree of freedom (lumped) model of the beam is built by means of Galerkin decomposition. The results provided by the lumped model are verified through comparison with the numerical data obtained by the Finite Differences method. In the framework of the lumped model, the stability properties of the beam are described using the canonical damped Mathieu equation. It was found that within the range of the frequencies below the fundamental frequency of the beam a frequency region always exists such that parametric resonance is possible for the excitation voltages below the critical voltage, corresponding to the Euler buckling of the beam.*

1 INTRODUCTION

Micro- and nanoelectromechanical systems (MEMS and NEMS) find applications in various areas of research and engineering due to their small size, low fabrication cost, unique performance and suitability for integration in complex functional systems [1]. Since the first micromachined electrostatically actuated resonator was introduced by Natanson [2], a large variety of MEMS/NEMS resonators was reported including radio frequency (RF) timing devices and filters [3], inertial sensors [4, 5] as well as mass [6, 7, 8] and stress [9] based sensors for chemical and biological detection. Resonant sensors benefit from the dependence of a device spectral characteristics on device parameters, the latter of which can be extracted with very high accuracy by tracking the changes in the resonant frequency.This principle lies in the foundation of resonant mass sensors [10].

Emerging of new applications and unabated progress in required performance of the devices motivates development of robust architectures for efficient resonant driving. Particularly, efficient parametric excitation, first reported for mechanical microstructures in nineties [11, 12], continues to attract considerable research attention in the realm of MEMS and NEMS as reflected in numerous publications (e.g., see reviews [13, 14] and references therein). Parametric excitation and parametric resonance (PR) are associated with the excitation through time-modulation of the parameters of the system rather than through direct force application to the structure [15]. These systems are distinguished by time-dependent effective stiffness or inertia coefficients of the governing equation and are described by (linear or nonlinear) Mathieu differential equations [15]. Parametrically excited sensors are attractive for a broad range of applications such as mass sensors [16], angular rate sensors [17, 18]) and scanning micro mirrors [19] thanks to their general characteristics of relatively wide bands of operation frequencies, large amplitudes and sharp transition between low-amplitude to high-amplitude response. In MEMS/NEMS devices parametric excitation is typically achieved through controlled modulation of effective stiffness of the mechanical system. In electrostatic devices, the actuation forces are usually nonlinear, time- and configuration-dependent functions, which affect the device effective stiffness [19, 20, 21, 22, 23, 24, 25, 26] and result in parametric excitation of the structures. Recently, parametric excitation has been demonstrated in MEMS/NEMS devices through various rich possibilities, including kinematic excitation of a beam's attachment point [27], direct mechanical stiffness modulation [28], the mass-matrix modulation [29, 30]) and via fringing electrostatic fields [16, 19, 31].

Joule heating of micro structures was considered mainly in the framework of the analysis of electro thermal actuators (e.g., see [32, 33]). Since the characteristic time associated with heating and cooling is typically much longer than the period of free vibrations of these structures, mainly static or low frequency operation of thermal actuators was explored. Some approaches were suggested addressing this intrinsic limitation [34]. Electrothermal heating (by a steady time-independent current) was suggested as an efficient way of tuning the resonant responses of electrostatically actuated devices [35, 36, 37]. Downscaling of the devices's dimensions reduces significantly the thermal response times and allows achieving of resonant thermal excitation of nanoelectromechanical (NEMS) devices using optical heating by means of modulated laser [38, 39, 40, 41]. Parametric excitation and parametric amplification in laser-heated micro beams was reported in [42, 43]. Laser heating was used also for the tuning of the resonant responses of nano beams [44]. Self-excitation of NEMS structures undergoing steady laser irradiation and optomechanical coupling was analyzed as well [38, 45, 46].

In this work we explore a simple but unusual way to excite resonant parametric vibrations of

a slender double clamped beam by means of thermoelectric excitation. Specifically, the modulation of the effective stiffness of the structure is achieved by changing the axial force through the time-periodic heating of the beam's material. An alternating electrical current passing through the beam results in the resistive Joule's heating of the beam's material and in appearance of the time-dependent axial compressive force. Note that combined thermal and magnetic actuation of micro beams was demonstrated theoretically and experimentally in [47]. In the present work we eliminate the magnetic Lorentz force and consider the case of excitation solely by heating. The main goal of the work is to investigate the feasibility of excitation of PR in the beam by means od Joule's heating.

2 FORMULATION

The device under consideration consists of a prismatic double clamped beam with length, width and thickness of L, b and h respectively, Fig. 1. The beam is assumed to be made of a linearly elastic material with the Young's modulus E and mass density ρ. The beam is free to deflect in the $\hat{x}\hat{z}$ (or $\hat{y}\hat{z}$) plane while the ends of the beam are constrained in both lateral $\hat{y},\ \hat{z}$ and axial $\hat{x}$ directions by unmoveable anchors attached to the substrate. The voltage difference V is applied between the anchors of the beam resulting in the current I passing through the beam.

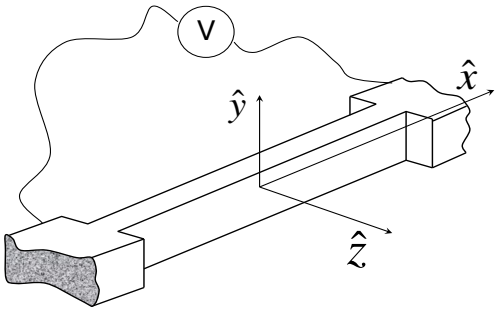

Figure 1: Model of a beam heated by an electric current.

The beam is described in the framework of the Euler-Bernoulli theory and under the assumption that the deflections, while comparable with the thickness of the beam, are small with respect to the beam's length. In addition, we assume that the axial and rotary inertia are negligible compared with the transverse inertia. Under these assumptions, the governing equation of the beam is (e.g., see [48] for the details of the development)

$$\rho A\frac{\partial^2 \hat{w}}{\partial \hat{t}^2} + \hat{c}\frac{\partial \hat{w}}{\partial \hat{t}} + EI_{yy}\frac{\partial^4 \hat{w}}{\partial \hat{x}^4} - \hat{N}\frac{\partial^2 \hat{w}}{\partial \hat{x}^2} = 0 \tag{1}$$

It is completed by homogeneous boundary conditions $\hat{w}(0,\hat{t}) = \hat{w}(L,\hat{t}) = 0,\ \partial\hat{w}(0,\hat{t})/\partial\hat{x} = \partial\hat{w}(L,\hat{t})/\partial\hat{x} = 0$. In Eq. (1) $\hat{x}$ and $\hat{t}$ are dimensional coordinate and time, respectively; A and I_{yy} are the cross-sectional area and the sectional second moment of area; $\hat{w}$ - is the deflection of the beam in the lateral $\hat{z}$ direction; $\hat{c}$ is coefficient of viscous damping. The axial tensile force

$$\hat{N} = \sigma_0 A - \frac{EA}{L}\int_0^L \alpha T\, d\hat{x} + \frac{EA}{2L}\int_0^L \left(\frac{d\hat{w}}{d\hat{x}}\right)^2 d\hat{x} \tag{2}$$

incorporates three terms: the time-independent tensile pre-load $\sigma_0 A$ (e.g., originated in the residual stress arising during the fabrication process), compressive force associated with the thermal stress and the nonlinear, deflection-dependent stretching force. In Eq. (2) $T = T(\hat{x}, \hat{t})$ is the temperature change above a reference temperature and $\alpha = \alpha(T)$ is the (generally speaking temperature-dependent [49]) coefficient of thermal expansion. Note that $T(\hat{x}, \hat{t})$ represents the temperature averaged across the section of the beam [32].

To simplify matters, in this work we adopt an assumption that the coefficient of the thermal expansion α is independent on temperature. In this case Eq. (1) can be written in the form

$$\hat{N} = \sigma_0 A - \frac{EA}{L}\alpha\bar{T} + \frac{EA}{2L}\int_0^L \left(\frac{d\hat{w}}{d\hat{x}}\right)^2 d\hat{x} \tag{3}$$

Here $\bar{T} = \bar{T}(\hat{t})$ is the temperature averaged along the beam. Equation (1) with the axial force given by Eq. (3) shows that changing of the temperature periodically in time will result in a time-dependent axial force. Consequently, Eq. (2) is an homogeneous partial differential equation with a time-dependent coefficient and is of a parametric type. By choosing the frequency and amplitude of the axial force within an appropriate interval, one can anticipate that it could be possible to excite parametric resonance in the beam.

3 Thermal problem

Electric potential difference is applied between the beam's ends. The heat (per unit volume of the beam's material) generated by the electric current is $E_{gen} = J^2\rho_e$ [32]. Here $J = J(x, y, z) = I/A$ is the current density and ρ_e is the electrical resistivity of the beam's material. This Joule's heating is assumed to be the only source of heat generation in the system under consideration while the influence of the thermoelastic coupling arising due to the heat generation associated with the rates of material deformation, is neglected.

For the sake of simplicity, in the analysis of the thermal problem we assume that the material parameters - thermal conductivity, specific heat and resistivity - are independent on temperature. Note that while in reality the temperature dependence of both thermal (conductivity, specific heat) and electrical (resistivity) parameters is significant, this assumption allows to obtain closed-form solutions and is often used in order to simplify development (e.g.,see [50]). In addition, we assume that the current density is distributed uniformly across the section of the beam. Finally, we neglect the term associated with the heat losses to the surrounding fluid and the substrate [51] through the beam's envelope and assume that the cooling of the beam takes place solely through its ends via the conductivity mechanism. Under these assumptions, the heat conduction in the beam can be described by the one-dimensional equation (e.g., see [32] for the reduction of the three-dimensional heat conductance problem to the one-dimensional counterpart)

$$\frac{d}{d\,\hat{t}}(\rho\, C_p\, T) = \frac{\partial}{\partial\,\hat{x}}\left(\kappa\frac{\partial\, T}{\partial\,\hat{x}}\right) + J^2\rho_e \tag{4}$$

Here $T(\hat{x})$ is the temperature (temperature excess above an ambient reference T_∞) averaged across the section of the beam, C_P is the specific heat, κ is the thermal conductivity and ρ is the material density. Note that in Eq. (4) the term $J^2\rho_e$ is the heat generated per unit length of the beam.

The voltage (and consequently the current) applied to the beam's ends contains both steady

V_{dc} and time-periodic V_{ac} components

$$J^2\,\rho_e = \frac{1}{\rho_e\,L^2}\left[V_{dc}^2 + \frac{V_{ac}^2}{2} + 2V_{dc}V_{ac}\cos(\hat{\omega}\,\hat{t}) + \frac{V_{ac}^2}{2}\cos(2\hat{\omega}\hat{t})\right] \tag{5}$$

Here $\hat{\omega}$ is an circular frequency of the driving electrical signal.

First we solve an auxiliary problem of the uniform (in space) harmonic heat source $W\ \cos(\hat{\omega}\hat{t})$. In this case in view of the adopted assumptions, Eq. (4) takes the form

$$\rho\,C_p\,\frac{\partial\,T}{\partial\,\hat{t}} = \kappa\frac{\partial^2\,T}{\partial\,\hat{x}^2} + W\ \cos(\hat{\omega}\,\hat{t}) \tag{6}$$

subject to the boundary conditions $T(\pm\,L/2,\hat{t})\ =\ 0$. For convenience, we introduce non-dimensional quantities

$$x = \frac{\hat{x}}{L},\quad t = \hat{\omega}\hat{t},\quad \theta = \frac{T\kappa}{W\,L^2},\quad \beta = L\sqrt{\frac{\rho\,C_p\hat{\omega}}{2\kappa}} \tag{7}$$

and re-write eq. (6) in the form

$$2\beta^2\,\frac{\partial\theta}{\partial t} = \frac{\partial^2\theta}{\partial x^2} + \cos\,(t) \tag{8}$$

with the boundary conditions $\theta(\pm\,1/2,t)\ =\ 0$. Note that the non-dimensional frequency parameter β represents the ratio between the beam's length to the thermal diffusion length $\mu = \sqrt{2k/(\rho\,C_p\hat{\omega})}$, which can be viewed as a characteristic dimension in the frequency domain, for the case of periodic heating [52].

We are looking for the solution in the following form

$$\theta(t,x) = \theta_s(x)\sin\,(t) + \theta_c(x)\cos\,(t) \tag{9}$$

Substituting of Eq. (9) into Eq. (8) yields the following system of ordinary differential equations for $\theta_s(x)$ and $\theta_c(x)$

$$\left\{\begin{array}{l} 2\beta^2\,\theta_s - \theta_c'' = 1 \\ 2\beta^2\,\theta_c + \theta_s'' = 0 \end{array}\right. \tag{10}$$

completed by the boundary conditions $\theta_s\ =\ \theta_c\ =\ 0$ at $x\ =\ \pm\,1/2$. Hereafter $(\ )'\ =\ d/dx$ or $(\ )'\ =\ \partial/\partial x$. The solution of the system is

$$\theta_s\ =\ \frac{1}{2\beta^2}\left[1-\frac{\cosh(\beta(x-1/2))\cos(\beta(x+1/2))+\cosh(\beta(x+1/2))\,\cos(\beta(x-1/2))}{\cosh(\beta)+\cos(\beta)}\right] \tag{11}$$

$$\theta_c\ =\ -\frac{1}{2\beta^2}\left[\frac{\sinh(\beta(x-1/2))\,\sin(\beta(x+1/2))+\sinh(\beta(x+1/2))\,\sin(\beta(x-1/2))}{\cosh(\beta)+\cos(\beta)}\right] \tag{12}$$

Averaging of $\theta(x,t)$, Eq. (9) over the length of the beam yields

$$\bar{\theta} = \int\limits_{-1/2}^{1/2}\theta(x,t)dx = \bar{\Theta}\cos(t-\phi) \tag{13}$$

where

$$\bar{\Theta}(\beta) = \frac{1}{2\beta^2}\left[\left(1-\frac{\sinh\beta+\sin\beta}{\beta(\cosh\beta+\cos\beta)}\right)^2+\left(\frac{\sinh\beta-\sin\beta}{\beta(\cosh\beta+\cos\beta)}\right)^2\right]^{\frac{1}{2}} \tag{14}$$

$$\phi(\beta) = \arctan\left(\beta\frac{\cosh\beta+\cos\beta}{\sinh\beta-\sin\beta}-\frac{\sinh\beta+\sin\beta}{\sinh\beta-\sin\beta}\right) \tag{15}$$

are the (frequency-dependent) amplitude and the phase, respectively. Note, that in the quasi-static case when $\beta \to 0$ we have

$$\theta_c = \frac{1}{8}-\frac{x^2}{2}, \quad \theta_s = 0, \quad \bar{\Theta} = \frac{1}{12} \text{ and } \phi = 0 \tag{16}$$

where $\bar{\Theta} = \sqrt{\bar{\Theta}_s^2+\bar{\Theta}_c^2}$ is the amplitude, $\phi = \arctan\left(\bar{\Theta}_s/\bar{\Theta}_c\right)$ is the phase and $\bar{\Theta}^s,\ \bar{\Theta}_c$ are the amplitudes $\theta_s,\ \theta_c$ averaged over the length of the beam.

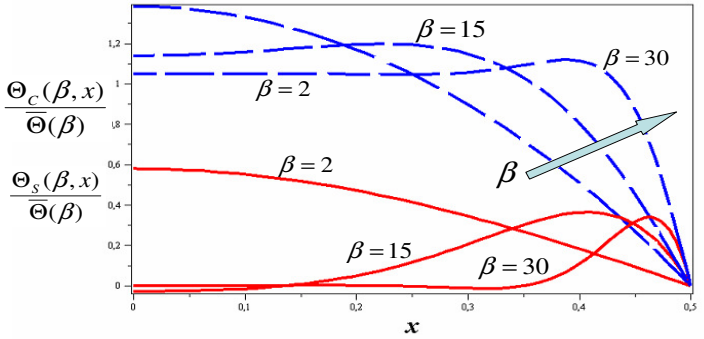

Figure 2: Non-dimensional temperature distribution along the beam: normalized amplitudes $\theta_s(x)$ and $\theta_c(x)$ (solid red and dashed blue lines, respectively) for $\beta = 2, 15$ and 30.

Figure 2 shows the distribution of the sine and cosine components of the temperature for differing values of β (different frequencies). For small β the distribution of the temperature is similar to the quasi-static case. With increase of the frequency, the space dependence of the temperature is less pronounced. The reason for this behavior is that at higher frequencies the diffusion length decreases and heat distribution becomes more local [53], which, combined with uniform heat generation along the beam, results in the temperature distribution close to uniform and justifies the spatial averaging for the case of high frequency excitation. Equation (14) suggests that the amplitude of temperature decreases as $1/2\beta^2$ with the increase of the frequency. Following combination of the solutions for the two limit cases (static and high frequency) allows simple approximation for the $\bar{\Theta}(\beta)$

$$\bar{\Theta}(\beta) \approx \left(\left(\frac{1}{12}\right)^{-1}+\left(\frac{1}{2\beta^2}\right)^{-1}\right)^{-1} = \frac{1}{12}\left(\frac{1}{1+\beta^2/6}\right) \tag{17}$$

The comparison of the approximation (17) with the exact averaged solution $\bar{\Theta}(\beta)$ is illustrated in Fig. 3.

In the case of Joule's heating, the heat propagation in the beam is described by Eq. (4) with the source therm $J^2\rho_e$ given by Eq. (5). Because of linearity of the problem, the temperature

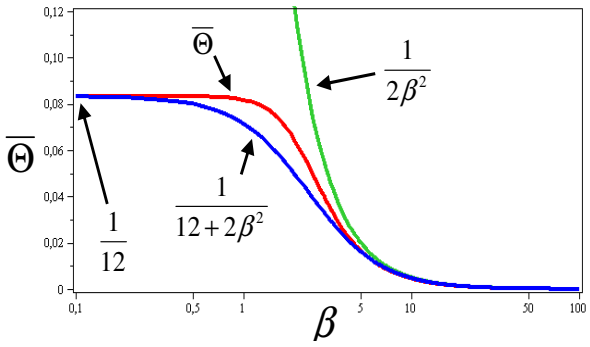

Figure 3: Amplitude $\bar{\Theta}$ of the temperature averaged over the beam's length (red curve) and its approximations for different values of β.

distribution in the beam can be represented as superposition of solutions Eq. (13) obtained for the case of harmonic heating

$$T = \frac{V_{dc}^2 + \frac{1}{2}V_{ac}^2}{8k\rho_e}\left[1 - 4x^2\right] + \frac{2\,V_{dc}\,V_{ac}}{k\rho_e}[\theta_c(x,\beta)\cos t + \theta_s(x,\beta)\sin t] + \\ + \frac{V_{ac}^2}{2k\rho_e}[\theta_c(x,\beta\sqrt{2})\cos 2t + \theta_s(x,\beta\sqrt{2})\sin 2t] \tag{18}$$

where $\theta_s(x,\beta)$ and $\theta_c(x,\beta)$are given by Eqs. (11) and (12). Using Eqs.(13)-(16) we calculate the temperature averaged along the length of the beam

$$\bar{T} = \frac{V_{dc}^2 + V_{ac}^2/2}{12k\rho_e} + \frac{2\,V_{dc}\,V_{ac}}{k\rho_e}\bar{\Theta}(\beta)\cos(t - \phi(\beta)) + \frac{V_{ac}^2}{2k\rho_e}\bar{\Theta}(\beta\sqrt{2})\cos(2t - \phi(\beta\sqrt{2})) \tag{19}$$

Note that Eq. (19) can be simplified for the case of large β (high frequency), when $\phi(\beta) \to \pi/2$, $\bar{\Theta}(\beta) \to 1/2\beta^2$ and $\bar{\Theta}(\beta\sqrt{2}) \to 1/4\beta^2$

$$\bar{T} = \frac{V_{dc}^2 + V_{ac}^2/2}{12k\rho_e} + \frac{V_{dc}\,V_{ac}}{k\rho_e\beta^2}\sin(t) + \frac{V_{ac}^2}{8k\rho_e\beta^2}\sin(2t) \tag{20}$$

In order to estimate the accuracy of the approximate analytical solution the numerical solution of the thermal problem Eq. (4) with the source therm $J^2\rho_e$ given by Eq. (5) was build by means of the finite differences method. The partial differential equation (4) completed by the zero temperature initial conditions and zero boundary conditions is reduced to the system of ordinary differential equations using a spacial finite difference discretization. The integration of the resulting system of linear ordinary differential equations in time is then carried out using fourth-order Runge-Kutta method implemented in Matlab [54]. In all the calculations presented hereafter we used the parameters listed in Table 1 until otherwise is stated. The nodal (discrete) values of the temperature are used for the calculation of the averaged (along the beam) temperature on each time step of the calculation. Figure 4 shows the the analytical steady-periodic and the numerical transient solutions in terms of the average temperatures. Good agreement between the two is observed. One can mention also that in accordance with Eq. (5) the source term $J^2\rho_e$ combines both double and single electrical signal frequencies. Figure 4 illustrates that the increase of the ratio V_{dc}/V_{ac} results in more pronounced response at the (single) frequency of the supplied electrical signal.

Table 1: Parameters of the structure and material properties used in calculations.

Notation	Parameter	Value	Unit
L	Beam's length	2000	μm
b	Beam's width	25	μm
h	Beam's thickness	8	μm
E	Young's modulus	169	GPa
ρ	Density	2330	kg/m^3
α	Thermal linear expansion coefficient	3E-6	$[^\circ C^{-1}$
C_p	Heat capacity	700	$J/kg\,K$
κ	Thermal conductivity	150	$W/\mathrm{m}K$
ρ_e	Electrical resistivity	0.0015	Ω·m

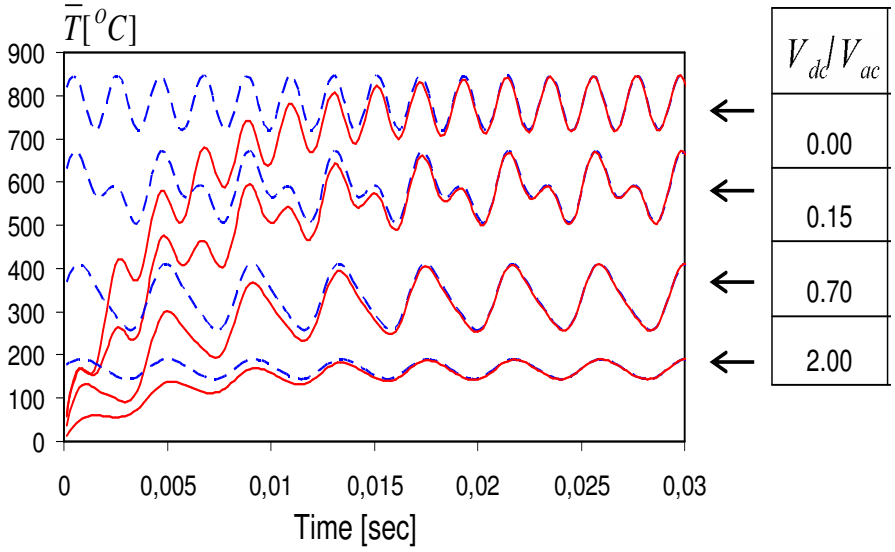

Figure 4: Comparison of the steady-periodic analytical and transient numerical solutions in terms of the average temperature of beam. In the case of dominant V_{ac}, relative to V_{dc}, the double frequency response is dominant. Beam dimensions and material properties correspond to listed in Table 1.

4 Coupled problem and decomposition

The dynamics of the beam heated by a time-dependent current are described by Eq. (1) with the axial force N given by Eq. (3), where the temperature $\bar{T}$, averaged along the length of the beam, is given by Eq. (19). By introducing the non-dimensional quantities

$$x = \frac{\hat{x}}{L}, \quad t = \hat{t}\sqrt{\frac{EI}{\rho A L^4}}, \quad \omega = \hat{\omega}\sqrt{\frac{\rho\, A\, L^4}{EI}} \quad w = \frac{\hat{w}}{r}, \quad c = \hat{c}\sqrt{\frac{EI\rho A}{L^4}} \tag{21}$$

where $r = \sqrt{I/A}$ is the cross-sectional gyration radius, we re-write eq. (1) in the form

$$w^{IV} + c\dot{w} - Nw'' + \ddot{w} = 0 \tag{22}$$

where $\dot{(\,)} = \partial/\partial t$. Note that in accordance with Eq. (21) the frequency was re-scaled. The non-dimensional axial force N is given by the expression

$$N = \gamma_0 + \gamma_1 \cos(\omega\, t - \phi(\beta)) + \gamma_2 \cos(2\omega\, t - \phi(\beta\sqrt{2})) + \frac{1}{2}\int_0^1 (w')^2\, dx \tag{23}$$

where the parameters associated with the driving terms are

$$\gamma_0 = \eta^2 \left[\varepsilon_0 - \frac{\alpha}{k\rho_e}\frac{V_{dc}^2 + V_{ac}^2/2}{12}\right], \quad \gamma_1 = -\frac{2\eta^2\alpha}{k\rho_e} V_{dc} V_{ac} \bar{\Theta}(\beta), \quad \gamma_2 = -\frac{\eta^2\alpha}{2k\rho_e} V_{ac}^2 \bar{\Theta}(\beta\sqrt{2}), \tag{24}$$

Here $\eta = L/r$ is the non-dimensional slenderness ratio of the beam and $\varepsilon_0 = \sigma_0/E$ is an initial tensile strain associated with the residual stress in the beam.

We use Galerkin decomposition in order to construct a single DOF (lumped) model of the beam. By substituting the approximation of the deflection $w = q(t)\psi(x)$ (where $\psi(x)$ is the base function) into eq. (23) we obtain

$$m\,\ddot{q} + c\,m\,\dot{q} + \left[k_B + \gamma_0\, k_S + \gamma(t)\, k_S + \frac{1}{2}\, k_S^2\, q^2\right] q = 0; \tag{25}$$

where

$$m = \int_0^1 \psi^2 dx; \;\; k_S = \int_0^1 (\psi')^2 dx; \;\; k_B = \int_0^1 (\psi'')^2 dx; \tag{26}$$

Equation. (24) suggests that γ_0 decreases with increasing of the electric current. It means that heating reduces the system stiffness, as expected. Note also that γ_0 can be negative and it is limited by the static buckling of the beam. The post buckling behavior is not considered in this work.

5 Static stability

When the axial force engendered by the Joule's heating became higher than the critical Euler's value, the beam becomes unstable and can buckle. The condition of the static instability can be obtained by requiring that the linearized counterpart of the stiffness term in Eq. (25) is zero

$$k_B + k_S\gamma_0 = 0 \tag{27}$$

For convenience, we replace $V_0^2 = V_{dc}^2 + V_{ac}^2/2$ in γ_0, Eq. (25). In analysis of the static buckling we use the buckling mode of the beam $\psi = (1 - \cos 2\pi\, x)/2$ as the base function. Taking into consideration that in this case the integrals m, k_S and k_B, Eq. (26), have the values of $3/8, \pi^2/2$ and $2\pi^4$, respectively we obtain the buckling criterion of the beam

$$\gamma_0 < -4\pi^2 \text{ or } V_0 > \sqrt{\frac{12k\rho_e(4\pi^2 + \eta^2\varepsilon_0)}{\alpha\eta^2}} \tag{28}$$

In the framework of the single DOF nonlinear lumped model, the equilibrium of the beam is described by the equation

$$k_B + k_S\gamma_0 + \frac{1}{2}\, k_S^2\, q^2 = 0 \tag{29}$$

Equation (29) suggests that deflection of the buckled beam is bounded due to the presence of the geometric non-linearity. The non-dimensional and dimensional midpoint deflections of the beam in the post-buckling configuration are as follows (see [55])

$$q^2 = \frac{\alpha\,\eta^2}{3\pi^2\, k\rho_e} V_0^2 - 16 - \frac{4\eta^2}{\pi^2}\varepsilon_0 \text{ and } \hat{q}^2 = \frac{\alpha\, L^2}{3\pi^2\, k\rho_e} V_0^2 - \frac{4t^2}{3} - \frac{4L^2}{\pi^2}\varepsilon_0 \tag{30}$$

where $\hat{q}$ is dimensional midpoint deflection. Note that this result can be obtained by replacing the prescribed axial compressive force by γ_0 in the exact solution for the buckled beam obtained in [55]. Figure 5 illustrates the comparison between the numerical finite differences (blue cycles) and analytical (red line) results for the static bifurcation of the silicon beam with the dimensions listed in Table 1 and without pre-stress (i.e., $\varepsilon_0 = 0$). The critical value of the voltage was found to be $V_{cr} \approx 5.9V$.

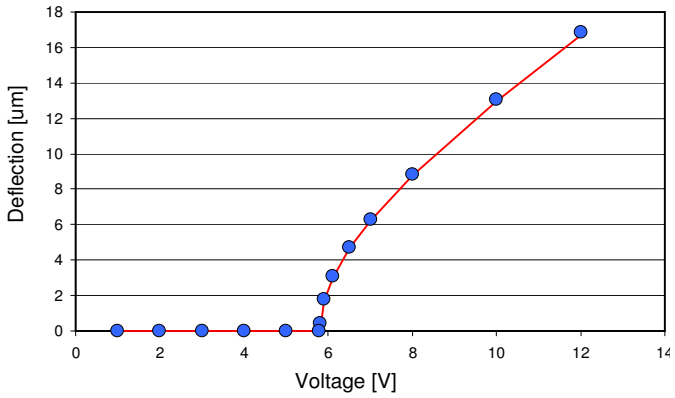

Figure 5: Buckling curves of the beam: comparison between the numerical finite differences (blue cycles) and analytical (red line) solutions describing the static bifurcation of the beam.

6 Parametric excitation

The ordinary differential equation (25) governing the beam's dynamics in the framework of the single DOF model is actually a particular case of a well-known damped Hill's equation (e.g.,see [15]) with an additional nonlinear cubic term. The time-periodic stiffness coefficient contains two time scales-one is proportional to the driving frequency ω (the frequency of the supplied electrical signal) and the second is twice of this frequency, i.e., 2ω. In order to examine the possibility of the PR in the beam under consideration, we reduce Eq. (25) to the form of a canonical Mathieu equation. First, we consider the case of the excitation solely by the ac voltage/current and $V_{dc} = 0$. In this case $\gamma_1(t) = 0$ and the time-dependent coefficient contains only one time scale associated with the excitation at the frequency 2ω. Next, since the parametric instability onset occurs at the straight undeformed configuration of the beam, we neglect the nonlinear cubic term in the equation. In addition, we assume that the beam is initially stress-free, which is typical of the single crystal Si devices considered in this work. By setting the phase lag ϕ (Eq. (19)) to be zero in a homogeneous equation, the single DOF model of the beam takes the form

$$m\ddot{q} + c\,m\dot{q} + [k_B + k_S\gamma_0 + k_S\gamma_2 \cos 2\omega\, t]\, q = 0; \tag{31}$$

where

$$\gamma_0 = -\frac{1}{24}\eta^2 \frac{\alpha}{k\rho_e} V_{ac}^2, \qquad \gamma_2 = -\frac{1}{2}\eta^2 \frac{\alpha}{k\rho_e} V_{ac}^2 \bar{\Theta}. \tag{32}$$

Here the amplitude of the temperature modulation $\bar{\Theta}$ is given by Eq. (14) with β replaced by $\beta\sqrt{2}$ (see Eq. (19)). Note that for convenience, we express the frequency parameter β in terms

of the non-dimensional frequency ω, defined in Eq. (21)

$$\beta = \sqrt{\frac{r\, C_p\, \omega}{2k}\sqrt{\rho\, E}} \tag{33}$$

By re-scaling time $t = \tau/2\omega$ in Eq. (31) we obtain

$$\frac{d^2q}{d\tau^2} + \frac{c}{2\omega}\frac{dq}{d\tau} + \frac{q}{4m\omega^2}\left[k_B - k_S\frac{1}{24}\eta^2\frac{\alpha}{k\rho_e}V_{ac}^2 + k_S\frac{1}{2}\eta^2\frac{\alpha}{k\rho_e}V_{ac}^2\bar{\Theta}\,\cos\tau\right] = 0. \tag{34}$$

This equation is actually the canonical Mathieu equation

$$\frac{d^2u}{d\tau^2} + \tilde{c}\frac{du}{d\tau} + (\delta + \epsilon\,\cos\tau)u = 0 \tag{35}$$

whose two coefficients –δ and ϵ– define the character of the response. The $\delta - \epsilon$ plane is subdivided into two sub-regions corresponding to the "stable" and "unstable" responses. The parametric resonance is possible for the values of δ and ϵ located within the "unstable" region. The location of the boundaries of the unstability region corresponding to the primary parametric resonance is given by the expression [15] (note that this approximation is valid for small ϵ)

$$\epsilon = \sqrt{4\left(\delta - \frac{1}{4}\right)^2 + \tilde{c}^2} \tag{36}$$

In accordance with Eq. (36) the parametric resonance in the damped Mathieu equation is possible for the values of ϵ higher than a certain threshold value (i.e. for $\epsilon > \tilde{c}$ in the case of primary PR [15]).

By comparing Eqs. (34) and (35) it is possible to express the parameters δ and ϵ in terms of the physical parameters of the beam

$$\tilde{c} = \frac{c}{2\omega}, \quad \epsilon = \frac{1}{8m\omega^2}k_S\eta^2\frac{\alpha}{k\rho_e}V_{ac}^2\bar{\Theta}, \quad \delta = \frac{1}{4m\omega^2}\left[k_B - k_S\frac{1}{24}\eta^2\frac{\alpha}{k\rho_e}V_{ac}^2\right] \tag{37}$$

On the other hand, in the beam under consideration, the parameters δ and ϵ are not independent and related through Eq. (37)

$$\epsilon = 12\bar{\Theta}\left(\frac{k_B}{4m\omega^2} - \delta\right) \tag{38}$$

Recall that in Eq. (38) $\bar{\Theta} = \bar{\Theta}(\beta)$, i.e., $\bar{\Theta}$ depends on the excitation frequency, as suggested by Eqs. (14), (33).

Figure 6 shows the location of the stability boundaries given by Eq. (36) on the $\delta - \epsilon$ plane and the lines $\epsilon = \epsilon(\delta)$ given by Eq. (38) each corresponding to a specific prescribed value of the driving frequency ω. Parameters of the beam correspond to listed in Table 1. Note that the frequency dependence of the location of the stability boundaries is due to the dependence of the damping term $\tilde{c}$ in the Mathieu equation on the driving frequency, Eq. (37). One observes that the parametric excitation is possible when the (non-dimensional) driving frequency is lower than a certain threshold value $\omega < \omega_{th} < 5.4$. Note that the natural frequency of the beam with no axial force is $\omega_0 = 4.73^2 = 22.39 >> \omega_{th}$. If the beam is excited at the frequencies above the threshold frequency the excitation of the PR can not be achieved.

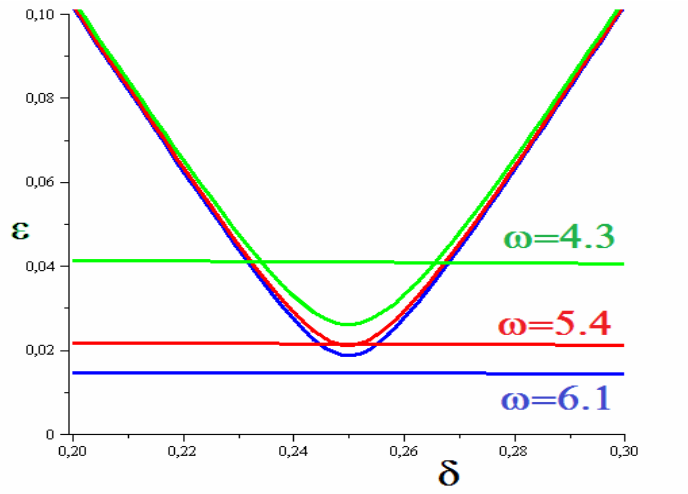

Figure 6: Boundaries Eq. (36) of the stability regions of the damped Mathieu equation. Straight lines $\epsilon = \epsilon(\delta)$, Eq. (38)represent the states of the system corresponding to a constant driving frequency. Parameters of the beam are listed in Table 1, Q-factor is 100.

7 CONCLUSIONS

In this work we investigate the feasibility of the excitation of the parametric resonance by means of time-periodic Joule's heating of double-clamped micro beam. The approach is distinguished by its simplicity and robustness and can be used, for example, in resonant sensors. In thermal micro actuators based on Joule's heating, the characteristic time constants corresponding to heating and cooling are typically much larger than the periods of free or resonant vibrations of micro structures. Our results suggest that in the system under consideration the excitation of PR is possible when the driving frequency (the frequency of the electric potential applied to the ends of the beam) is lower than a certain threshold value. For the parameters of the beam used in calculations and for the case of excitation by the ac voltage, this value was found to be significantly lower than the natural frequency of the beam. This result has a clear physical interpretation. The PR is excited when the frequency of the stiffness modulation, which is in our case the frequency of the temperature fluctuation in the beam, is close to twice the natural frequency. For the given dimensions and material (mechanical and electrical) properties of the structure the achievable "thermal" frequency is limited by the heating/cooling characteristics times and cannot be increased. However, the frequency of the PR cane be pushed down. Joule heating by a time-periodic voltage/current results in appearance of a steady component of the temperature. This steady heating of the beam leads to the appearance of a steady compressive axial force and results in the decrease of the natural frequency of the beam to the required value close to the half of the temperature modulation frequency. Heating allows the decrease of the frequency of the beam to any value below its natural frequency down to zero value, which corresponds to the buckling of the beam. Our results show that a combination of a driving voltage and of the driving frequency can be always found such that the PR frequency is decreased to the value of the driving frequency.

Acknowledgments The research is supported by the consortium PARM-2, FP7-PEOPLE-2011-IAPP, Marie Curie Actions, project no. 284544.

REFERENCES

[1] M. Tanaka, An industrial and applied review of new MEMS devices features. *Microelectronic Eng.,* 84, 1341–1344, 2007

[2] H. C. Nathanson, W. E. Newell, R. A. Wickstrom, and J. R. Davis, The resonant gate transistor. *IEEE Trans. Electron. Devices,* **14** 117-133, 1967.

[3] G. M. Rebeiz, *RF MEMS : Theory Design and Technology.* Hoboken N J : Wiley-Interscience, 2003.

[4] N. Yazdi, F. Ayazi, K. Najafi, Micromachined inertial sensors. *Proceedings of The IEEE* textbf86(8), 1640–1659, 1998.

[5] C. Acar, A. M. Shkel, *MEMS Vibratory Gyroscopes: Structural Approaches to Improve Robustness.* Springer, New York, 2009.

[6] X. M. H. Huang, M. Manolidis, Jun Seong Chan and J. Hone, Nanomechanical hydrogen sensing. *Appl. Phys. Letters*, **86**, 143104, 2005.

[7] B. Ilic, H. G. Craighead, S. Krylov, W. Senaratne, C. Ober, and P. Neuzil Attogram detection using nanoelectromechanical oscillators. *J. Appl. Phys.* **95** 3694-3703, 2004.

[8] B. Ilic, Y. Yang, K. Aubin, R. Reichenbach, S. Krylov, and H. G. Craighead, Enumeration of DNA molecules bound to a nanomechanical oscillator. *Nano Letters,* **5**, 925–929, 2005.

[9] D. J. Joe, Y. Linzon, V. P. Adiga, R. A. Barton, M. Kim, B. R. Ilic, S. Krylov, J. M. Parpia, and H. G. Craighead, Stress-based Resonant Volatile Gas Microsensor Operated near the Critically-buckled State. *Journal of Applied Physics*, **111**(10), pap. 104517 2012.

[10] N. Lobontiu, *Mechanical Design of Microresonators: Modeling and Applications.* McGraw-Hill Nanoscience and Technology, 2005.

[11] D. Rugar and P. Grùtter, *Phys. Rev. Lett.* **67**, 699, 1991.

[12] K. L. Turner, S. A. Miller, P. G. Hartwell, N. C. MacDonald, S. H. Strogatz, and S. G. Adams, Five parametric resonances in a micromechanical syste. *Nature*, **36**, 149–152, 1998.

[13] R. Lifshitz, and M. C. Cross, Nonlinear dynamics of nanomechanical and micromechanical resonators. *Review of Nonlinear Dynamics and Complexity*, Heinz Georg Shuster Ed Wiley-VCH Verlag GmbH & Co KGaA Weinheim, Vol 1 1-52, 2008.

[14] J. Rhoads, S. W. Shaw, K. L. Turner, Nonlinear dynamics and its applications in micro- and nanoresonators. *Proc. DSCC2008 2008 ASME Dynamic Systems and Control Conference October 20-22 Ann Arbor Michigan USA* pap. DSCC2008–2406, 2008.

[15] R. H. Rand, *Lecture Notes on Nonlinear Vibrations, Version 52*, Retrieved from http://audiophile.tam.cornell.edu/randdocs/nlvibe52.pdf, (2005)

[16] W. Zhang, and K. L. Turner, Application of parametric resonance amplification in a single-crystal silicon micro-oscillator based mass sensor. *Sens. Act. A*, **122**, 23-30, 2005.

[17] L. A. Oropeza-Ramos, C. B. Burgner, K. L. Turner, Robust micro-rate sensor actuated by parametric resonance. *Sensors and Actuators A* **152** 80-87, 2009.

[18] Z. Hu, B. J. Gallacher, K. M. Harish, J. S. Burdess, An experimental study of high gain parametric amplification in MEMS. *Sensors and Actuators A* **162** 145-154, 2010.

[19] C. Ataman, O. Kaya, H. Urey, Analysis of parametric resonances in comb-driven microscanners. *Proc. Conf. on MEMS MOEMS and Micromachining Apr. 29-30 2004 Strasbourg France Proc. of The Society Of Photo-Optical Instrumentation Engineers (SPIE)* Vol. 5455, 128–136, 2004.

[20] M. Napoli, R. Baskaran, K. L. Turner, and B. Bamieh, Understanding mechanical domain parametric resonance in microcantilevers. *Proc. IEEE Sixteenth Int. Annual Conference on MEMS (MEMS' 2003)*, 169–172, 2003.

[21] S. Krylov, I. Harari, and Y. Cohen, Stabilisation of electrostatically actuated microstructures using parametric excitation. *J. Micromech. Microeng.,* **15**, 1188–1204, 2005.

[22] J. F. Rhoads, S. W. Shaw, and K. L. Turner, The nonlinear response of resonant microbeam systems with purely-parametric electrostatic actuation. *J. Micromech. Microeng.,* **16**, 890-899, 2006.

[23] J. F. Rhoads, S. W. Shaw, and K. L. Turner, J. Moehlis, B. E. DeMartini, W. Zhang, Generalized parametric resonance in electrostatically actuated microelectromechanical oscillators. *J. Sound Vib.,* **296**, 797-829. 2006.

[24] S. Krylov, Parametric excitation and stabilization of electrostatically actuated microstructures. *Int. J. for Multiscale Comput. Eng.*, **6**(6), 563–584, 2008.

[25] R. M. C. Mestrom, R. H. B. Fey, J. T. M. van Beek, K. L. Phan, and H. Nijmeijer, Modelling the dynamics of a MEMS resonator: Simulations and experiments. *Sens. Act. A*, **142**, 306-315, 2008.

[26] C. van der Avoort, R. van der Hout, J. J. M. Bontemps, P. G. Steeneken, K. Le Phan, R. H. B. Fey, J. Hulshof, J. T. M. van Beek, Amplitude saturation of MEMS resonators explained by autoparametric resonance. *J. Micromech. Microeng.,* **20**, (10), Article-Number 105012, 2010.

[27] A. Vyas, D. Peroulis, A. K. Bajaj, A Microresonator Design Based on Nonlinear 1 : 2 Internal Resonance in Flexural Structural Modes. *Journal of Microelectromechanical Systems*, **18**, No. 3, 744–762, 2009.

[28] S. Krylov, Y. Gerson, T. Nahmias, U. Keren, Excitation of large amplitude parametric resonance by the mechanical stiffness modulation of a microstructure. *J. Micromech. Microeng*., **20**, pap. 015041 2010.

[29] D. Schwartz, D.J. Kim, R.T. MCloskey, Frequency tuning of a disk resonator gyro via mass matrix perturbation. *J. Dyn. Syst. Control* 131 pap. 061004, 2009.

[30] S. Krylov, K. Lurie, A. Ya'akobovitz, Compliant structures with time-varying moment of inertia and non-zero averaged momentum and their application in angular rate microsensors. *Journal of Sound and Vibrations*, **330**, 4875-4895, 2011.

[31] S. Krylov, N. Molinazzi, T. Shmilovich, U.Pomerantz, S. Lulinsky, Parametric excitation of flexural vibrations of micro beams by fringing electrostatic fields. *Proc. ASME Design Engineering Technical Conference IDETC/CIE2010*, v 4, 601–611, 2010.

[32] J. A. Pelesko and D. H. Bernstein *Modeling of MEMS and NEMS.* London-New York-Washington DC: Chapman&Hall A CRC Press Company, 2002.

[33] V. Kaajakari, *Practical MEMS.*, Small Gear Publishing, 2009.

[34] R. Mahameed, D. Elata, Two-dimensional analysis of temperature-gradient actuation of cantilever beam resonators. *J. Micromech. Microeng.*, **15**, 1414–1424, 2005.

[35] T. Remtema, L.Lin, Active frequency tuning for micro resonators by localized thermall stressing effects. *Sensors and Actuators A*, **91**, 326–332, 2001.

[36] Ki Bang Lee, A. P. Pisano, L. Lin, Nonlinear behaviors of a comb drive actuator under electrically induced tensile and compressive stresses. *J. Micromech. Microeng*. **17** 557-566, 2007.

[37] Seong Chan Jun, Hyungbin Son, C.W. Baik, J.M. Kim, S.W. Moon, H. Jin Kim, X.M.H. Huang, J. Hone, Electrothermal noise analysis in frequency tuning of nanoresonators. *Solid-State Electronics*

[38] K. Aubin, M. Zalalutdinov, A. Tuncay, R. B. Reichenbach, R. H. Rand, A. T. Zehnder, J. Parpia, H. G. Craighead, Limit cycle oscillations in CW laser driven NEMS. *J. Microelectromech. Syst.,* **13**, 1018-1026, 2004.

[39] B. Ilic, S. Krylov, K. Aubin, R. Reichenbach, and H. G. Craighead, Optical excitation of nanoelectromechanical oscillators. Appl. Phys. Lett. **86**, 193114, 2005.

[40] B. Ilic, S. Krylov, and H. G. Craighead, Theoretical and Experimental Investigation of Optically Driven Nanoelectromechanical Oscillators," *Journal of Applied Physics*, **107**, 034311, 2010.

[41] M. Pandey, K. Aubin, M. Zalalutdinov, R. B. Reichenbach, A. T. Zehnder, R. H. Rand, H. G. Craighead, Analysis of frequency locking in optically driven MEMS resonators. *J. Microelectromech. Syst.*, **15**, 1564–1554, 2006.

[42] M. Zalalutdinov, A. Olkhovets, A. T. Zehnder, B. Ilic, D. Czaplewski, H. G. Craighead, J. M. Parpia, Optically pumped parametric amplification for micromechanical oscillators. *Appl. Phys. Letters*, **78**, 3142–3144, 2001

[43] T. Sahai, R. B. Bhiladvala, A. T. Zehnder, Thermomechanical transitions in doubly-clamped micro-oscillators. *Int. J. Non-Lin. Mech.*, **42**, 596–607, 2007.

[44] T. Sahai, R. B. Bhiladvala, A. T. Zehnder, Thermomechanical transitions in doubly-clamped micro-oscillators., *International Journal of Non-Linear Mechanics*. **42**, 596 - 607, 2007.

[45] D. Blocher, A. T. Zehnder, R. H. Rand, S. Mukerji, Anchor deformations drive limit cycle oscillations in interferometrically transduced MEMS beams. *Finite Elements in Analysis and Design*, **49**, 52-57, 2012.

[46] S. Zaitsev, O. Gottlieb, E. Buks, Nonlinear dynamics of a microelectromechanical mirror in an optical resonance cavity. *Nonlinear Dynamics*, **69**, 1589-1610, 2012.

[47] D. Schreiber, S. Krylov, Y. Shacham-Diamand, T. Sibgatullin, Electromagnetic microactuators with on-chip resin-bonded permanent magnets. *Proc. of the 9th Biennial ASME Conference on Engineering Systems Design and Analysis ESDA08*, July 7-9, 2008, Haifa, Israel

[48] P. Villagio, *Mathematical Models for Elastic Structures*. Cambridge University Press, Cambridge, 1997.

[49] Y. Okada, and Y. Tokumaru, Precise determination of lattice parameter and thermal expansion coefficient of silicon between 300 and 1500 K. *J. Appl. Phys*. **56**, 314–320, 1984.

[50] R. Hickey, D. Sameoto, T. Hubbard and M. Kujath, Time and frequency response of two-arm micromachined thermal actuators. *J. Micromech. Microeng.* **13,** () 40-46, 2003.

[51] Qing-An Huang and Neville Ka Shek Lee, Analysis and design of polysilicon thermal flexure actuator. *J. Micromech. Microeng*. **9** 64-70, 1999.

[52] E. Marin,Characteristic dimensions for heat transfer.*Lat. Am. J. Phys. Educ.*,**4**,56–60, 2010.

[53] H.S. Carslaw and J.C. Jaeger, *Conduction of heat in Solids*. 2nd ed. Oxford: Clarendon Press, 1986.

[54] L. Shampine, M. Reichelt, The Matlab ODE suite. *SIAM J. Sci. Comput.,* **18**, 1–22, 1997.

[55] A. H. Nayfeh, S. Emam, Exact solution and stability of postbuckling configurations of beams. *Nonlinear Dynamics*,**54**, 395–408, 2008.